Journal of Physics D:
Applied Physics

PAPER

Tungsten oxide ion-gated phototransistors using ionic liquid and aqueous gating media

To cite this article: Gabriel Vinicius De Oliveira Silva *et al* 2019 *J. Phys. D: Appl. Phys.* **52** 305102

IOP Publishing Journal of Physics D: Applied Physics

J. Phys. D: Appl. Phys. **52** (2019) 305102 (9pp) https://doi.org/10.1088/1361-6463/ab1dbb

Tungsten oxide ion-gated phototransistors using ionic liquid and aqueous gating media

Gabriel Vinicius De Oliveira Silva[1,2,7], Arunprabaharan Subramanian[3,7], Xiang Meng[1,7], Shiming Zhang[3], Martin S Barbosa[1,4], Bill Baloukas[1], Daniel Chartrand[5], Juan C Gonzáles[2], Marcelo Ornaghi Orlandi[4], Francesca Soavi[6], Fabio Cicoira[3] and Clara Santato[1,8]

[1] Département de Génie physique, Polytechnique Montréal, C.P. 6079, Succ. Centre-ville, Montréal (QC) H3C 3A7, Canada
[2] Departamento de Física, Universidade Federal de Minas Gerais, Belo Horizonte, Minas Gerais (MG), 30123-970, Brazil
[3] Département de Génie chimique, Polytechnique Montréal, C.P. 6079, Succ. Centre-ville, Montréal (QC) H3C 3A7, Canada
[4] Departamento de Físico-Química, Universidade Estadual Paulista, Rua Professor Degni, 55, Araraquara, 14800-060, Brazil
[5] Département de Chimie, Université de Montréal, C. P. 6128, Succ. Centre-ville, Montréal (QC) H3C 3J7, Canada
[6] Dipartimento di Chimica Giacomo Ciamician, Università di Bologna, Via Selmi 2, Bologna 40126, Italy

E-mail: clara.santato@polymtl.ca

Received 24 February 2019, revised 11 April 2019
Accepted for publication 29 April 2019
Published 23 May 2019

Abstract

Ion-gated transistors employ ionic gating media (e.g. ionic liquids, polymer electrolytes, aqueous saline solutions) to modulate the density of the charge carriers in the transistor channel. Not only they operate at low voltages (ca 0.5–1 V) but they can also feature printability, flexibility and easy integration with chemo- and bio-sensing platforms. Metal oxides are transistor channel materials interesting for their processability in air, at low temperature. Among metal oxides, tungsten oxide (band gap ca 2.5–2.7 eV) stands out for its electrochromic, gas sensing and photocatalytic properties. Here we demonstrate ion-gated tungsten oxide transistors and phototransistors working in different ion gating media, such as one hydrophobic ionic liquid and an aqueous electrolyte, fabricated both on rigid and flexible substrates. Ion-gated tungsten oxide phototransistors operating in aqueous media could be used as photocatalytic sensors in portable applications.

Keywords: ionic liquids, tungsten oxide, ion-gated transistors, phototransistors, polyimide

S Supplementary material for this article is available online

(Some figures may appear in colour only in the online journal)

Introduction

Metal oxides are applied in a broad range of technologies, such as electrochromic windows, batteries, gas sensors and photoelectrochemical cells [1–5]. They are used as transistor channel materials for technologies such as active matrix displays, due to their ease of process in air and at low temperature, charge carrier mobility, uniformity and transparency [6–12].

Ion-gated transistors (IGTs) employ ionic gating media (e.g. ionic liquids, polymer electrolytes, aqueous saline

[7] These authors equally contributed to this work.
[8] Author to whom any correspondence should be addressed.

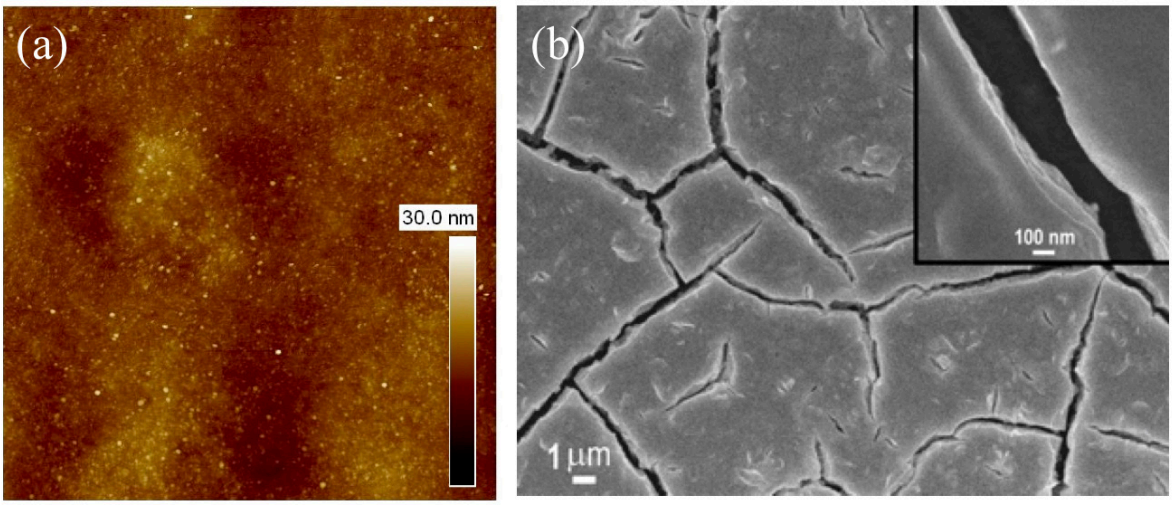

Figure 1. WO_3 films on PI treated at 300 °C. (a) 5 μm × 5 μm AFM topographical image and (b) SEM image (5 kV). The AFM image has been taken in a crack-free portion of the film.

solutions) to modulate the density of the charge carriers in the transistor channel. In IGTs, the high capacitance featured by the ion gating medium/transistor channel interface (ca 1–10 μF cm^{-2}) leads to high charge carrier density (10^{14}–10^{15} cm^{-2}), bringing about low-voltage operation (sub 1 V) [13–17]. Besides this last advantage, IGT-based technologies are interesting in terms of printability, flexibility, and easy integration with chemo- and bio-sensing platforms.

Phototransistors are optoelectronic devices that combine the switching and amplifying functions typical of transistors with light response (photocurrent). Phototransistors are used in light sensing devices, security systems and computer logic circuitry [18]. In phototransistors, the density of charge carriers can be modulated not only by the electrical bias applied to the gate electrode (conventional transistor modulation) but also by the illumination conditions. Several metal oxides are used in phototransistors, namely IGZO, ZnO, TiO_2 and CuO (see table s1). [19–23] Among metal oxides, tungsten oxide (bandgap ~2.5–2.7 eV) stands out for its application in smart windows, gas sensors and photocatalysis [2]. This oxide can be easily processed by various techniques, including sol-gel [24, 25].

We recently demonstrated ionic liquid (1-ethyl-3-methylimidazolium bis(trifluoromethylsulfonyl)imide ([EMIM][TFSI]))-gated transistors making use of channels of polycrystalline films of tungsten oxide [26]. We observed that the doping process of the channel takes place by a combination of electrostatic and electrochemical mechanisms, paralleled by a structural transformation of the metal oxide from the monoclinic to the orthorhombic crystal structure. To extend the technological potential of tungsten oxide IGTs, we explore their operation under suitable illumination conditions (ion-gated phototransistors). Tungsten oxide ion-gated phototransistors can be used as tools for a number of fundamental and applied studies. Besides the study of the combined effect of ion-gating and light exposure on the channel doping, their application as photocatalytic sensors, e.g. to monitor water quality in portable devices, is foreseen. In this last context, the processability of the transistors on lightweight plastic substrates would represent a clear benefit for the development of novel flexible sensing technologies [27, 28].

In this work, we report on ion-gated phototransistors based on tungsten oxide films deposited by the sol-gel method, on rigid (SiO_2/Si) and flexible (polyimide, PI) substrates. The films were investigated for their morphological, structural, optical and electrochemical properties by atomic force microscopy (AFM), scanning electron microscopy (SEM), x-ray diffraction (XRD), UV–vis spectroscopy and cyclic voltammetry, prior their characterization in transistor configuration. We used both the ionic liquid [EMIM][TFSI] and aqueous electrolyte solutions as the gating media for our transistors, which were characterized both in the dark and under solar light illumination conditions.

Results and discussion

Film characterization

Prior to device characterization, we gained insight on the morphological, structural and optical properties of the WO_3 films. We initially prepared the films on conventional rigid substrates (SiO_2/Si), and we treated them at 550 °C. Afterwards, we found the suitable conditions to fabricate transistor channel films on polyimide (PI), considering the limitations on the temperature of thermal treatment when overgrowing films on such polymer substrate, i.e. ca 300 °C. As expected, AFM, SEM and XRD indicate that the effect of the nature of the substrate and the temperature of the thermal treatment on the morphological and structural properties of the films is remarkable. AFM and SEM images of WO_3 films treated at 550 °C on SiO_2/Si show that WO_3 nanostructured films feature a smooth surface (figure s1 (stacks.iop.org/JPhysD/52/305102/mmedia)) [25, 26]. XRD patterns (not shown) confirm that these films have a monoclinic crystalline structure [26]. As opposed to nanostructured films on SiO_2/

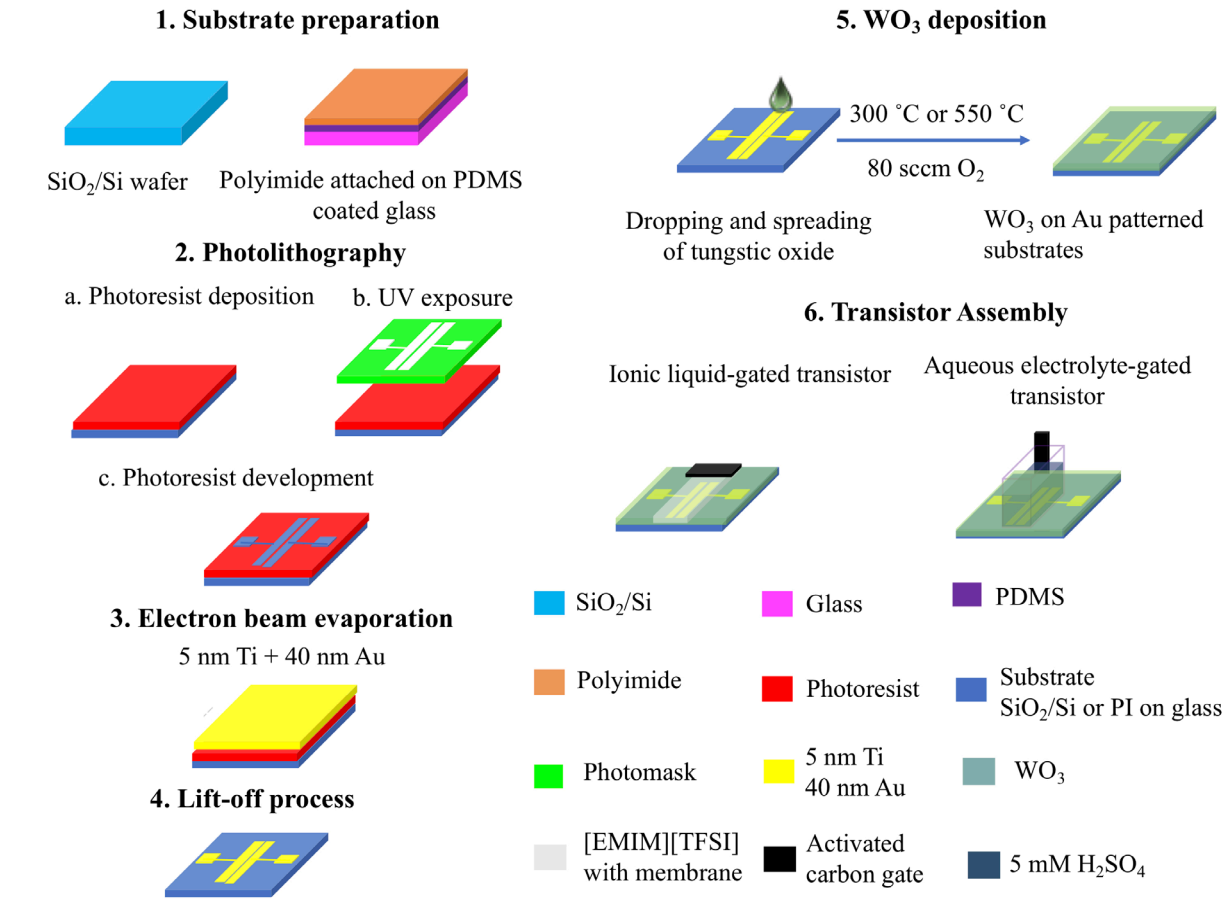

Figure 2. Process flow for the fabrication of transistors investigated in this work, gated with ionic liquids and aqueous electrolytes.

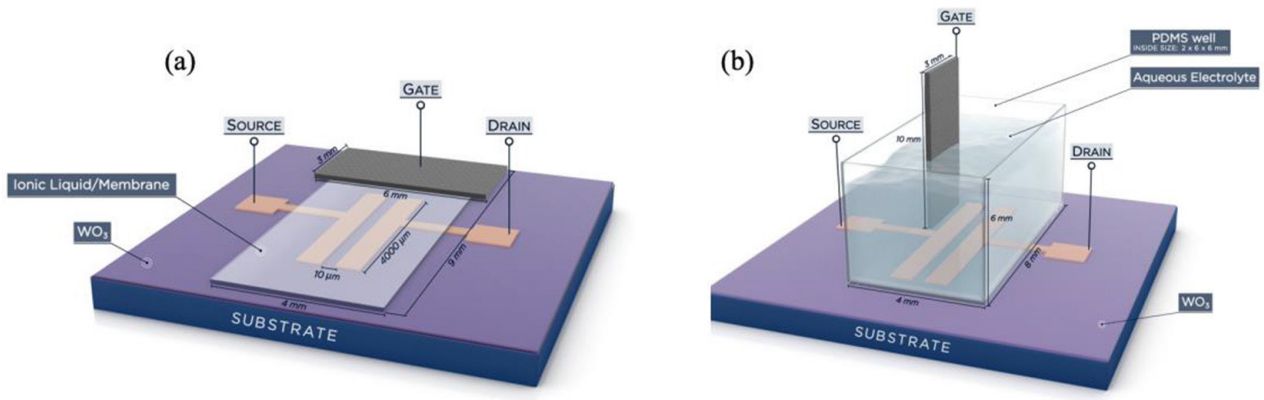

Figure 3. Device schemes of (a) ionic liquid-gated and (b) aqueous electrolyte-gated transistors investigated in this work.

Si treated at 550 °C, films on PI treated at 300 °C feature cracks (figure 1) that, nevertheless, do not prevent promising IGT performance (*vide infra*). From AFM images, we deduced a root mean square (rms) surface roughness of about 1.6 ± 0.4 nm in regions excluding the cracks, significantly lower than that of nanostructured films treated at 550 °C. XRD patterns (not shown) indicate that these films are amorphous. UV-visible spectra reveal that the visible light absorption starts at about 470 nm for films treated 550 °C and at about 435 nm for film treated at 300 °C (figure s2).

Ion-gated phototransistors based on WO_3 films treated at 550 °C on SiO_2/Si

Prior to transistor characterization, we studied the cyclic voltammetry behavior of the transistor channel material, on both SiO_2/Si and PI substrates (figures 2, 3 and s3). The voltammetry was carried out *in situ*, in transistor configuration. The channel material included between source and drain electrodes acted as the working electrode and the high surface area (1000–2000 $m^2\ g^{-1}$) activated carbon paper, featuring a specific capacitance of 100–200 $F\ g^{-1}$, as both the counter and

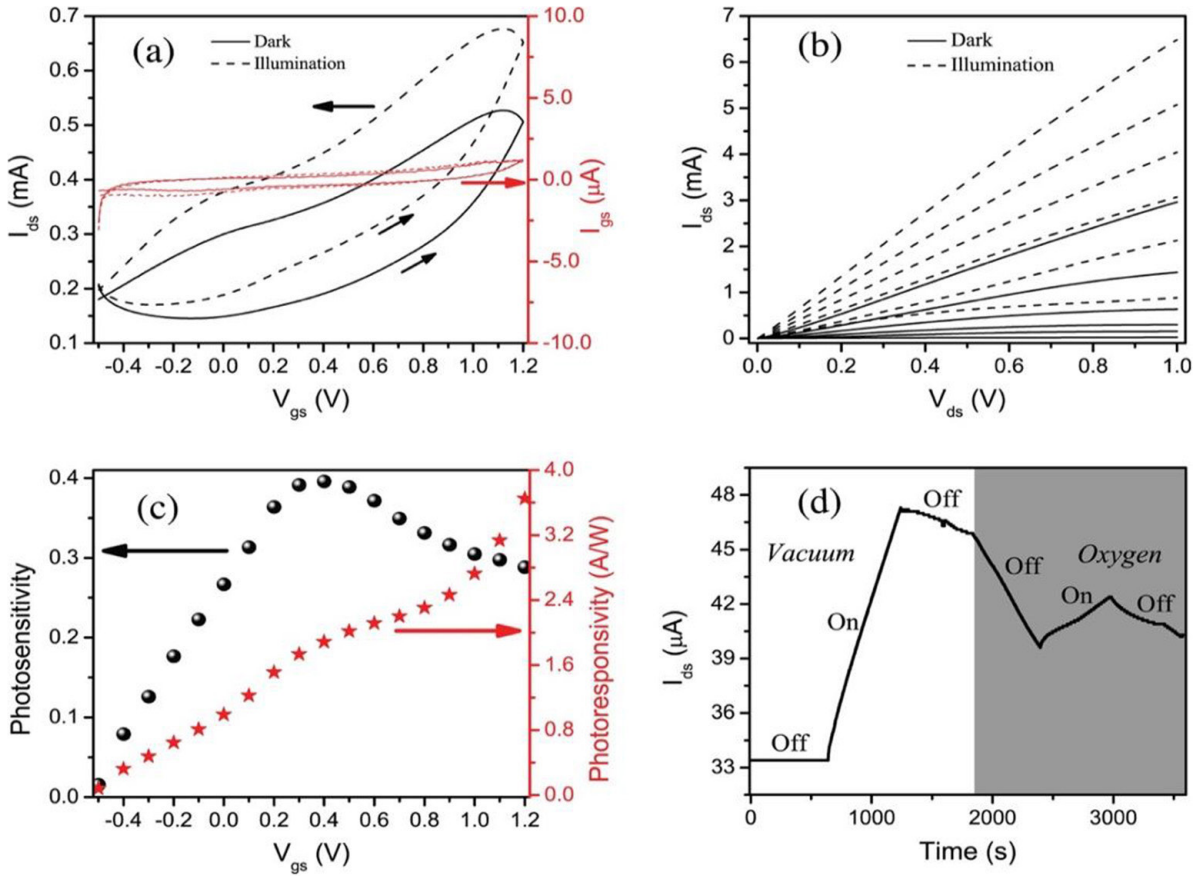

Figure 4. [EMIM][TFSI]-gated phototransistors based on WO_3 films treated at 550 °C on SiO_2/Si. (a) Transfer characteristics at $V_{ds} = 0.2$ V, V_{gs} scan rate 1 mV · s^{-1}; dark (continuous) and illumination (dashed) conditions, under vacuum. (b) Output characteristics in the dark (continuous) and under illumination (dashed) conditions, $V_{gs} = 0$, 0.4, 0.6, 0.8, 1.0, 1.2 V, V_{ds} scan rate 1 mV · s^{-1}, in vacuum. (c) Photosensitivity and photoresponsivity versus V_{gs} at $V_{ds} = 0.2$ V. (d) Transient measurement under chopped light (time interval 600 s) at $V_{ds} = 0.2$ V and $V_{gs} = 0.1$ V, in vacuum (white region) and O_2 atmosphere (grey region).

quasi-reference electrode [29]. The voltammograms suggest that our IGTs can be safely operated within an interval of gate-source voltage (V_g) values included between −1.2 and +1.2 V. The transfer and output characteristics of transistors based on films treated at 550 °C, measured in the dark under vacuum, show a typical n-type behaviour (figures 4(a) and (b)). The linear transfer characteristics (source-drain voltage, V_{ds}, equal to 0.2 V) show a significant hysteresis, likely due to slow ionic transport during doping/dedoping of the films.

After the characterization in the dark, we measured the transistor characteristics under solar light illumination conditions. These confirmed that WO_3 films are photosensitive (the apparent threshold voltage, V_{th}, was 0.1 V in the dark and −0.1 V under illumination). We extracted the channel charge carrier density in the linear regime (p, charge carrier/cm^2) using the relationship $p = Q/e \cdot s = \left[\int (I_{gs} dV_{gs})\right] / [(dV_{gs}/dt) \cdot e \cdot s]$, where Q is the doping charge obtained by integrating the gate-source current, I_{gs}, versus time, t, during the forward scan of the transfer curves ($-0.5\ \text{V} < V_{gs} < 1.2\ \text{V}$), e is the elementary charge and s is surface area. A debate is still open on whether the geometric area (in our present case 0.36 cm^2, i.e. the area of membrane soaked with [EMIM][TFSI]) or the Brunauer–Emmett–Teller (BET) surface area (in our present case 10.6 cm^2 [26]) should be used for the calculation of the charge carrier density in IGTs presenting nanostructured channels. As this debate is off topic with respect to the present manuscript (that is the demonstration of tungsten oxide ion-gated phototransistors making use of rigid and flexible substrates, working in hydrophobic and aqueous media), we calculated the charge density using both the geometric and the BET surface areas. The characteristics of our devices are summarized in table s4(a) (values obtained using geometric area) and s4b (values obtained using BET surface area).

Using the geometric area, we obtained a charge carrier density of about 8×10^{15} in the dark and 1×10^{16} cm^{-2} under illumination. Density values obtained using the BET surface area were of 2.6×10^{14} in the dark and 3.3×10^{14} cm^{-2} under illumination. The electron mobility, μ, was then calculated in the linear regime according to the formula $\mu = L \cdot I_{ds}/(W \cdot e \cdot p \cdot V_{ds})$, where L is the transistor channel length (10 μm) and W is the channel width (4000 μm). Obviously, the approach adopted to choose the surface area s affected this calculation too (being the mobility calculated using the value of the charge carrier density). The obtained values were ca 5×10^{-3} cm^2 V^{-1} s^{-1}, both in dark and illumination conditions, when using the geometric area, and ca 0.15 cm^2 V^{-1} s^{-1} when using the BET surface area.

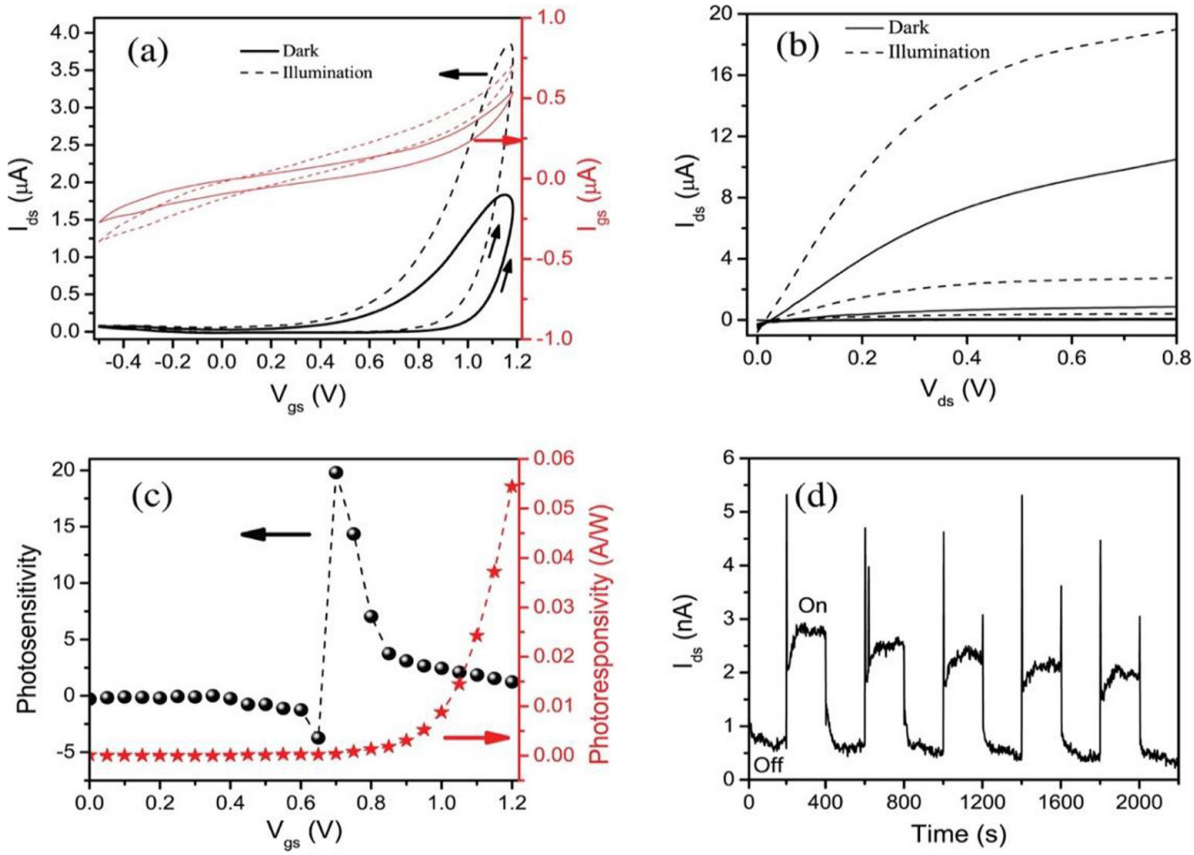

Figure 5. [EMIM][TFSI]-gated phototransistors based on WO_3 films treated at 300 °C on polyimide. (a) Transfer characteristics at $V_{ds} = 0.2$ V, V_{gs} scan rate 10 mV · s^{-1}; dark (continuous) and illumination (dashed) conditions, under vacuum. (b) Output characteristics in the dark (continuous) and under illumination (dashed) conditions, $V_{gs} = 0$, 0.4, 0.6, 0.8, 1.0, 1.2 V, V_{ds} scan rate 10 mV · s^{-1} under vacuum (c) photosensitivity and photoresponsivity versus V_{gs} at $V_{ds} = 0.2$ V. (d) Transient measurement under chopped light (time interval 200 s) at $V_{ds} = 0.2$ V and $V_{gs} = 0.1$ V under vacuum. With respect to 550 °C-treated films, the scan rate is here is higher (1 versus 10 mV · s^{-1}), likely due to the increased ion permeability of the films.

The performance of phototransistors can be expressed by two figures of merit, i.e. photosensitivity, $S = (I_{ds,\ light} - I_{ds,dark})/I_{ds,dark}$, and photoresponsivity, $R = (I_{ds,\ light} - I_{ds,dark})/P \cdot s$, where $I_{ds,\ dark}$ and $I_{ds,\ light}$ are the drain-source current under dark and light conditions, P is the power of the incident light and s is the geometric area of the channel (10 μm × 4000 μm = 0.0004 cm^2). In photosensitivity versus V_{gs} plots we observe a maximum at ca 0.35 V (figure 4(c)). At $V_{gs} =$ 0.35 V the transition between photodoping and electrochemical doping mode likely takes place. The dependence of the photosensitivity on V_{gs} can be exploited to control the light response of the phototransistors. The photoresponsivity as a function of V_{gs} shows an increase of about 45 times between $V_{gs} = -0.5$ V ($R = 0.08$ A W^{-1}) and 1.2 V ($R = 3.6$ A W^{-1}).

The photoresponsivity of transistors based on inorganic gating media (both conventional or high-κ) is generally higher than that of IGTs (table s1). Our values of the photoresponsivity are similar (table s2) to those reported in the literature for ion-gated phototransistors. Nevertheless, IGTs have the advantage to operate at lower voltages (see tables s1 and s3, the latter describing tungsten oxide-based photodetectors). Furthermore, it is worth noticing that the originality of our results is the demonstration of ion-gated phototransistors that have the potential to be used, when operated in aqueous media, as photocatalytic sensors for portable applications, based on the photocatalytic properties of tungsten oxide (*vide infra*, results on aqueous electrolytes).

The transient characteristics of WO_3 phototransistors in dark and light conditions reveal fundamental aspects of their operational behavior. The current in dark conditions increases by about 30% (from 33 to 47 μA) after 600 s-long light exposure (figure 4(d)). Surprisingly, the current remains almost unchanged (at ca 46 μA) after the light is switched off. This observation can be attributed to a phenomenon known as persistent photoconductivity (PPC). PPC, already reported for WO_3, is observed when the electrical conductivity under illumination persists after the removal of the illumination [30–33]. The PPC of our WO_3 films is dramatically reduced in O_2 atmosphere: a drop of the current of about 15% (from 46 to 40 μA) is observed in the dark, after 600 s. Upon light exposure in O_2 atmosphere for 600 s the current increases by ca 7% (from 40 to 43 μA). PPC, attributable to the absence of recombination paths at low O_2 concentrations, has to be carefully taken into account for practical applications of WO_3 phototransistors, e.g. as photosensors. [33]

Ion-gated phototransistors based on WO_3 films treated at 300 °C on polyimide

With the aim to develop flexible devices, we fabricated WO_3 phototransistors on plastic polyimide (PI) substrates (figures 2, 3(a) and 5). These devices featured ON/OFF ratio of ca 30 in the dark (extracted within the interval $-0.5\ \mathrm{V} < V_{gs} < 1.2\ \mathrm{V}$). This value is considerably higher than that observed for WO_3 films on SiO_2/Si treated at 550 °C (about 3) and is mainly ascribed to the lower I_{off} on polyimide. The apparent V_{th} changed from 0.8 V in the dark to 0.7 V under illumination. In the dark, we deduced a charge carrier density of ca 3×10^{14} cm^{-2} and a mobility of ca 5×10^{-4} $cm^2\ V^{-1}\ s^{-1}$ (for samples treated at 300 °C on PI we used the geometric area for the calculations of the density, considering the morphology of the samples). Under illumination, the ON/OFF ratio was ca 50, the charge carrier density 4×10^{14} cm^{-2} and the mobility ca 8×10^{-4} $cm^2\ V^{-1}\ s^{-1}$.

A maximum photosensitivity of ca 20 and photoresponsivity of ca 0.05 A W^{-1} were extracted (figure 5(c)). The photosensitivity versus V_{gs} plot shows that there is an interval of V_{gs} where the values of the photosensitivity are higher (between about 0.7 V and 0.8 V); this interval can be associated to the shift of the apparent V_{th} under illumination versus dark conditions. The high value of the photosensitivity constitutes a significant improvement with respect to the value obtained with films on SiO_2 and can be explained by the low value of the dark current. The photoresponsivity increases by a factor of ca 130 when V_{gs} increases from −0.5 V to 1.2 V. The transient characteristics of the WO_3 films on PI show that the photocurrent, after a spike followed by a gentle increase in the first seconds after the light is switched on, reaches a saturation value such that the current increase by ca 80% (from 0.5 to 2.5 nA) upon light exposure (figure 5(d)). WO_3 phototransistors on PI operated under vacuum conditions do not show PPC, in agreement with their lower surface area with respect to 550 C°- treated films [33].

Aqueous electrolyte-gated phototransistors with WO_3 films treated at 550 °C on SiO_2/Si

Considering that tungsten oxide in aqueous solutions is chemically stable at acidic pH, aqueous electrolyte-gated phototransistors were characterized using 5 mM H_2SO_4 as the gating medium (figures 2, 3(b) and 6) [34, 35]. Prior to the transistor characterization, the electrochemical characterization of the metal oxide films was carried out. We obtained the typical voltammograms of tungsten oxide in this environment, indicating the reduction of the tungsten oxide (n-type doping) paralleled by proton incorporation, ensuring film electroneutrality (figure s4). The device characteristics clearly show their photosensitivity. These transistors showed the ON/OFF current ratio of ca 8 and 9, in dark and illumination conditions, extracted for $0\ \mathrm{V} < V_{gs} < 0.8\ \mathrm{V}$. The apparent V_{th} changed from 0.4 V in the dark to 0.3 V under illumination. The photosensitivity and photoresponsivity of the 5 mM H_2SO_4-gated WO_3 phototransistors are shown in figure 6(c). A linear, gentle increase in photosensitivity was observed 0 V to 0.45 V_{gs}; after this value, the slope of the plot increased and the photosensitivity reached a quasi-plateau at ca $V_{gs} = 0.6$ V. A photoresponsivity values of ca 16 A W^{-1} was observed at 0.8 V; this value is 10 times higher than that observed at 0 V (1.6 A W^{-1}). Charge carrier density values of 6×10^{15} and 8×10^{15} cm^{-2} were observed in dark and illumination conditions, using the geometric area of the the PDMS well used to confine the electrolyte (0.12 cm^2, Experimental). The density values calculated using the BET surface area (3.5 cm^2, see Experimental) were 2×10^{14} cm^{-2} and 3×10^{14} cm^{-2}, in dark and illumination conditions. Values of the electron mobility of 1.3×10^{-2} and 1.7×10^{-2} $cm^2\ V^{-1}\ s^{-1}$ were extracted in dark and illumination conditions, using the geometric area. Values of 0.4 and 0.5 $cm^2\ V^{-1}\ s^{-1}$ were observed in dark and illumination conditions, using the BET surface area. There were no significant changes in the values of the charge carrier density and electron mobility, between dark and illumination conditions.

Conclusions

We demonstrated IGTs and phototransistors (illuminated with simulated solar light), based on sol-gel tungsten oxide films, capable to operate at about 1 V, making use of ionic liquid and, for the first time, aqueous electrolyte gating media. To develop, on the long term, lightweight and flexible technologies based on IG phototransistors for portable applications, the films were deposited on polyimide and thermally treated at 300 °C, a temperature compatible with that plastic substrate. At the fundamental level, work is in progress to evaluate the effect of the frequency of the illumination, scan rate of the electrical potential and advancement of the electrochemical doping (possibly paralleled by electrochromism) on the performance of the phototransistors. At the technological level, work is in progress to develop ion-gated tungsten oxide phototransistors working in aqueous gating media possibly including redox active chemicals from industrial effluents with the aim to use them to evaluate the quality of drinking water.

Experimental

Materials

$Na_2WO_4{\cdot}2H_2O$, ethanol and Dowex 50WX2 hydrogen form resin (100–200 mesh) were purchased from Sigma Aldrich. Polyethylene glycol 200 (PEG 200) was purchased from Fluka. The ionic liquid, 1-ethyl-3-methylimidazolium bis(trifluoromethylsulfonyl)imide ([EMIM][TFSI]) was purchased from IoLiTec, (purity >99%) and purified prior use under vacuum (ca 10^{-6} Torr) at 80 °C for 12 h. The purified ionic liquid was stored in a N_2 glovebox (H_2O and $O_2 \leqslant 7$ ppm) for a maximum of one day before use. Polyimide (PolyFLE™ XF-102) sheets (125 μm thick) were purchased from POLYONICS. The gate electrode for ionic liquid gating consisted of carbon paper (Spectracorp 2050, 6 mm × 3 mm) coated with high surface area carbon ink made of activated carbon powder (PICACTIF SUPERCAP BP10, Pica, 28 mg ml^{-1}) and polyvinylidene fluoride (PVDF, KYNAR

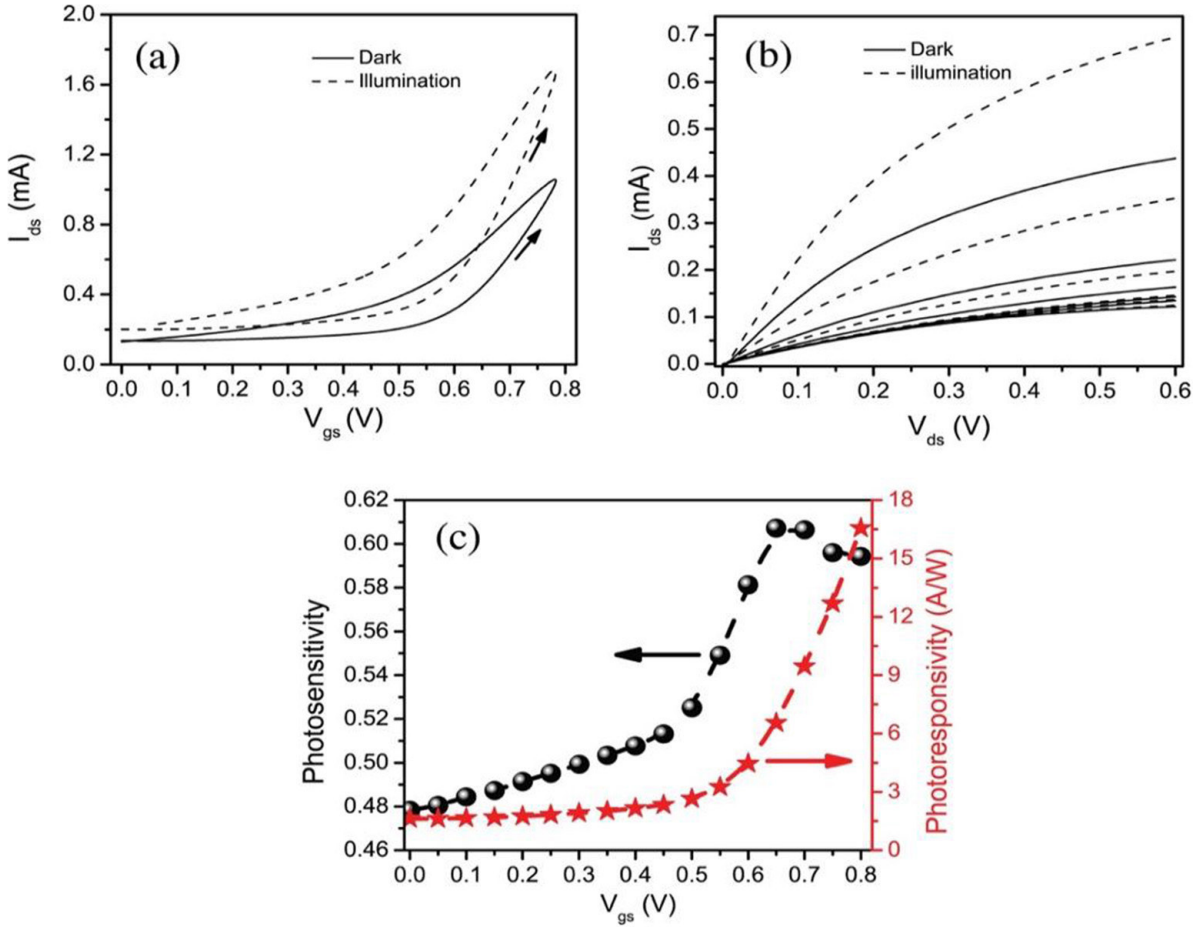

Figure 6. (a) Aqueous electrolyte (5 mM H_2SO_4)-gated phototransistors based on WO_3 films treated at 550 °C on SiO_2/Si. (a) Transfer characteristics at $V_{ds} = 0.2$ V, V_{gs} scan rate 10 mV · s^{-1}; dark (continuous) and illumination (dashed). (b) Output characteristics in the dark (continuous) and under illumination (dashed), $V_{gs} = 0$, 0.2, 0.3, 0.4, 0.5, 0.6 V, V_{ds} scan rate 10 mV · s^{-1}. (c) Photosensitivity and photoresponsivity versus V_{gs}, at $V_{ds} = 0.2$ V.

HSV900, 1.4 mg ml^{-1}) binder in the solvent N-methyl pyrrolidone (NMP, Fluka, >99.0%). The gate electrode for aqueous electrolyte consisted of carbon paper (Spectracorp 2050, 10 × 3 mm) coated with high surface area carbon ink made of activated carbon powder (PICACCHEM SUPERCAP BP9, Pica, 28 mg ml^{-1}) and Nafion (Sigma Aldrich, 1.4 mg l^{-1}) binder in the solvent isopropanol.

Microfabrication

Polyimide substrates were cleaned by sequential sonication in acetone, isopropyl alcohol (IPA), and deionized (DI) water (10 min for each step) and then dried using nitrogen flow. They were then laminated on a glass slide pre-covered with a 300 μm polydimethylsiloxane (PDMS) layer, to ensure substrate flatness during the following photolithography steps. Both SiO_2/Si and polyimide substrates were pre-patterned by photolithography with Ti/Au (5 nm/40 nm) source and drain electrodes (channel width, W, 4000 μm and length, L, 10 μm). Prior to deposition of the tungsten oxide precursor, the substrates were wet-cleaned again by sequential ultrasonic baths in IPA, acetone and IPA followed by N_2 drying and UV-ozone exposure for 15 min.

Film deposition

The films were deposited by casting the solution on the substrate and gently spreading it using a glass slide. The films were first dried at room temperature for 10 min, then thermally treated for 30 min at 550 °C (SiO_2/Si) and for 5 h at 300 °C (PI), in 80 sccm of O_2. Two sequential applications of the tungstic acid, each followed by a thermal treatment, were carried out on SiO_2/Si. A single application was carried out on PI.

Assembly of the electrolyte-gated transistors

A Durapore GVHP membrane filter (4 mm × 9 mm = 0.36 cm^2) soaked in the ionic liquid was placed on top of the tungsten oxide film constituting the transistor channel. Afterwards, the activated carbon paper gate electrode was placed beside the channel. The distance between the gate electrode and the channel was ca 0.5 mm. 5 mM H_2SO_4 electrolyte solution was prepared by diluting 17.8 M H_2SO_4 (Sigma Aldrich) of stock solution using deionized water. The electrolyte was confined in the transistor channel using PDMS well (2 × 6 × 6 mm) attached on the substrate. The gate electrode was immersed in the electrolyte solution during the measurements.

Characterization

AFM images were acquired in ambient conditions, in tapping mode, with a Digital Instruments Dimension 3100. Tapping mode was performed at a scan rate of 1 Hz using etched silicon cantilevers (ACTA from Applied Nanostructures, Inc.) with a resonance frequency around 300 kHz, a spring constant of 40 N m^{-1} and tip radius <10 nm. SEM was carried out using a JEOL 7500 equipped with a field-emission electron gun. XRD was performed by a Bruker D8 system with Cu Kα_1 and Cu Kα_2 sources. A Perkin Elmer LAMBDA 1050 spectrophotometer equipped with an integrating sphere was used to obtain the UV–visible spectra of tungsten oxide films deposited on quartz substrates. The electrochemical tests were performed using a PARSTAT 2273 (Princeton Applied Research) potentiostat in a N_2 glove box (H_2O and $O_2 \leqslant 7$ ppm). The optoelectronic characterizations were conducted by using a probe station connected to a semiconductor parameter analyzer (Agilent B1500A), at room temperature, in vacuum (ca 10^{-4} Torr). A solar simulator (SCIENCETECH SLB300A) with one sun illumination (100 mW cm^{-2}) was used to characterize the devices in illumination condition.

Acknowledgments

This work is financially supported by NSERC DG (C S and F C), MESI PSIIRI 936 (C S and F C) and China Scholarship Council (X M). M S B acknowledges FAPESP for financial aid (#2014/27079-9, #2015/50526-4 and #2016/09033-7) and LMA-IQ-UNESP for electron microscopy facilities. A S is grateful to the Trottier Energy Institute for a doctoral scholarship. We also benefited from FRQNT-RQMP support.

ORCID iDs

Clara Santato https://orcid.org/0000-0001-6731-0538

References

[1] Grätzel M 2001 Photoelectrochemical cells *Nature* **414** 338
[2] Deb S K 2008 Opportunities and challenges in science and technology of WO_3 for electrochromic and related applications *Sol. Energy Mater. Sol. Cells* **92** 245–58
[3] Granqvist C G 2000 Electrochromic tungsten oxide films: review of progress 1993–1998 *Sol. Energy Mater. Sol. Cells* **60** 201–62
[4] Ponzoni A, Comini E, Sberveglieri G, Zhou J, Deng S Z, Xu N S, Ding Y and Wang Z L 2006 Ultrasensitive and highly selective gas sensors using three-dimensional tungsten oxide nanowire networks *Appl. Phys. Lett.* **88** 203101
[5] Baeck S H, Choi K S, Jaramillo T F, Stucky G D and McFarland E W 2003 Enhancement of photocatalytic and electrochromic properties of electrochemically fabricated mesoporous WO_3 thin films *Adv. Mater.* **15** 1269–73
[6] Barquinha P, Pereira S, Pereira L, Wojcik P, Grey P, Martins R and Fortunato E 2015 Flexible and transparent WO_3 transistor with electrical and optical modulation *Adv. Electron. Mater.* **1** 1500030
[7] Garlapati S K, Divya M, Breitung B, Kruk R, Hahn H and Dasgupta S 2018 Printed electronics based on inorganic semiconductors: From processes and materials to devices *Adv. Mater.* **30** 1707600
[8] Xu W, Li H, Xu J-B and Wang L 2018 Recent advances of solution-processed metal oxide thin-film transistors *ACS Appl. Mater. Interfaces* **10** 25878–901
[9] Yang J T, Ge C, Du J Y, Huang H Y, He M, Wang C, Lu H B, Yang G Z and Jin K J 2018 Artificial synapses emulated by an electrolyte-gated tungsten–oxide transistor *Adv. Mater.* **30** 1801548
[10] Leng X, Pereiro J, Strle J, Dubuis G, Bollinger A, Gozar A, Wu J, Litombe N, Panagopoulos C and Pavuna D 2017 Insulator to metal transition in WO_3 induced by electrolyte gating *NPJ Quantum Mater.* **2** 35
[11] Altendorf S G, Jeong J, Passarello D, Aetukuri N B, Samant M G and Parkin S S 2016 Facet-independent electric-field-induced volume metallization of tungsten trioxide films *Adv. Mater.* **28** 5284–92
[12] Nishihaya S, Uchida M, Kozuka Y, Iwasa Y, Kawasaki M, Nishihaya S, Uchida M, Kozuka Y, Iwasa Y and Kawasaki M 2016 Evolution of insulator-metal phase transitions in epitaxial tungsten oxide films during electrolyte-gating *ACS Appl. Mater. Interfaces* **8** 22330–6
[13] Bisri S Z, Shimizu S, Nakano M and Iwasa Y 2017 Endeavor of iontronics: from fundamentals to applications of ion-controlled electronics *Adv. Mater.* **29** 1607054
[14] Xie W, Zhang X, Leighton C and Frisbie C D 2017 2D Insulator-metal transition in aerosol-jet-printed electrolyte-gated indium oxide thin film transistors *Adv. Electron. Mater.* **3** 1600369
[15] Leighton C 2019 Electrolyte-based ionic control of functional oxides *Nat. Mater.* **18** 13
[16] Barbosa M, Oliveira F M, Meng X, Soavi F, Santato C and Orlandi M 2018 Tungsten oxide ion gel-gated transistors: how structural and electrochemical properties affect the doping mechanism *J. Mater. Chem.* C **6** 1980–7
[17] Tarabella G, Mohammadi F M, Coppedè N, Barbero F, Iannotta S, Santato C and Cicoira F 2013 New opportunities for organic electronics and bioelectronics: ions in action *Chem. Sci.* **4** 1395–409
[18] Baeg K J, Binda M, Natali D, Caironi M and Noh Y Y 2013 Organic light detectors: photodiodes and phototransistors *Adv. Mater.* **25** 4267–95
[19] Ouyang W, Teng F, He J H and Fang X 2019 Enhancing the photoelectric performance of photodetectors based on metal oxide semiconductors by charge-carrier engineering *Adv. Funct. Mater.* **29** 1807672
[20] Kang B H, Kim W-G, Chung J, Lee J H and Kim H J 2018 Simple hydrogen plasma doping process of amorphous indium gallium zinc oxide-based phototransistors for visible light detection *ACS Appl. Mater. Interfaces* **10** 7223–30
[21] Hu L, Liao Q, Xu Z, Yuan J, Ke Y, Zhang Y, Zhang W, Wang G P, Ruan S and Zeng Y-J 2019 Defect reconstruction triggered full-color photodetection in single nanowire phototransistor *ACS Photonics* **6** 886–94
[22] Liu H-Y and Huang R-C 2018 A study of anatase TiO_2-Based thin film phototransistors by non-vacuum thin film deposition method *IEEE Trans. Electron Devices* **65** 2517–24
[23] Lee S, Lee W-Y, Jang B, Kim T, Bae J-H, Cho K, Kim S and Jang J 2018 Sol-gel processed p-type CuO phototransistor for a near-infrared sensor *IEEE Electron Device Lett.* **39** 47–50
[24] Livage J and Guzman G 1996 Aqueous precursors for electrochromic tungsten oxide hydrates *Solid State Ion.* **84** 205–11
[25] Santato C, Odziemkowski M, Ulmann M and Augustynski J 2001 Crystallographically oriented mesoporous WO_3 films:

synthesis, characterization, and applications *J. Am. Chem. Soc.* **123** 10639–49

[26] Meng X, Quenneville F, Venne F, Di Mauro E, Işık D, Barbosa M, Drolet Y, Natile M M, Rochefort D and Soavi F 2015 Electrolyte-gated WO_3 transistors: electrochemistry, structure, and device performance *J. Phys. Chem.* C **119** 21732–8

[27] Dang V Q, Trung T Q, Duy L T, Kim B-Y, Siddiqui S, Lee W and Lee N-E 2015 High-performance flexible ultraviolet (UV) phototransistor using hybrid channel of vertical ZnO nanorods and graphene *ACS Appl. Mater. Interfaces* **7** 11032–40

[28] Knobelspies S, Daus A, Cantarella G, Petti L, Münzenrieder N, Tröster G and Salvatore G A 2016 Flexible a-IGZO phototransistor for instantaneous and cumulative UV-exposure monitoring for skin health *Adv. Electron. Mater.* **2** 1600273

[29] Sayago J, Soavi F, Sivalingam Y, Cicoira F and Santato C 2014 Low voltage electrolyte-gated organic transistors making use of high surface area activated carbon gate electrodes *J. Mater. Chem.* C **2** 5690–4

[30] Huang K and Zhang Q 2011 Giant persistent photoconductivity of the WO_3 nanowires in vacuum condition *Nanoscale Res. Lett.* **6** 52

[31] Mondal S, Ram Ghimire R and Raychaudhuri A 2013 Enhancing photoresponse by synergy of gate and illumination in electric double layer field effect transistors fabricated on n-ZnO *Appl. Phys. Lett.* **103** 231105

[32] Jeon S, Ahn S-E, Song I, Kim C J, Chung U-I, Lee E, Yoo I, Nathan A, Lee S and Ghaffarzadeh K 2012 Gated three-terminal device architecture to eliminate persistent photoconductivity in oxide semiconductor photosensor arrays *Nat. Mater.* **11** 301

[33] Fàbrega C, Hernández-Ramírez F, Prades J D, Jiménez-Díaz R, Andreu T and Morante J R 2010 On the photoconduction properties of low resistivity TiO_2 nanotubes *Nanotechnology* **21** 445703

[34] Santato C, Ulmann M and Augustynski J 2001 Photoelectrochemical properties of nanostructured tungsten trioxide films *J. Phys. Chem.* B **105** 936–40

[35] Natan M J, Mallouk T E and Wrighton M S 1987 The pH-sensitive tungsten (VI) oxide-based microelectrochemical transistors *J. Phys. Chem.* **91** 648–54